JOURNAL OF CATALYSIS **121**, 165–173 (1990)

Studies on Ruthenium–Tin Boride Catalysts

I. Characterization

V. M. DESHPANDE, W. R. PATTERSON,*[,2] AND C. S. NARASIMHAN[1]

Alchemie Research Centre, P.O. Box 155, Belapur Road, Thane-400601, Maharashtra, India, and
**Chemicals & Polymers Group, Imperial Chemical Industries, P.O. Box 8, The Heath, Runcorn,*
Cheshire WA7 4QE, United Kingdom

Received August 15, 1988; revised May 2, 1989

A new mixed metal boride catalyst system, Ru–Sn–B, was prepared by reducing metal salts with sodium borohydride. The catalysts were also supported on γ-Al_2O_3. The supported as well as the unsupported catalysts were characterized by H_2 chemisorption, XRD, XPS, TEM/EDX, and SIMS techniques. Based on the available evidence from the various techniques, two types of surface species involving Ru, Sn, and B were suggested.

INTRODUCTION

Metal borides have been studied extensively as catalysts for hydrogenation reactions (*1–4*). Their catalytic activity is highly dependent upon the method of preparation. The activity and selectivity of NiB and CoB, for instance, can be altered significantly by varying the amount of metal-associated boron (*5–7*) as well as by adding promoter elements like Ru, Pt, Rh, Cr, and Mo (*8*). However, the literature is rather scarce on the characterization aspects of metal borides. In fact, there seems to be no study at all on the characterization of mixed metal boride systems.

Our studies on metal borides were initiated to explore the possibility of designing suitable metal or mixed metal boride catalysts for selective hydrogenation reactions. During this process, we prepared a new mixed metal boride catalyst, ruthenium–tin boride, which showed unique catalytic properties for reducing α,β-unsaturated aldehydes to unsaturated alcohols and fatty acid esters to fatty alcohols in high yields (*9, 10*). In this paper, we report detailed characterization of this new mixed metal boride system by H_2 chemisorption, XRD, XPS, TEM/EDX, and SIMS techniques to identify the nature of surface species present on the catalysts.

EXPERIMENTAL

Preparation of the Catalysts

Ru–Sn–B/γ-Al_2O_3. Appropriate quantities of aqueous solutions of $RuCl_3 \cdot 3H_2O$ and stannous chloride are mixed in a beaker. On addition of stannous chloride to the ruthenium chloride solution there was a color change, probably indicating reduction of Ru^{3+} to Ru^{2+} accompanied by oxidation of Sn^{2+} to Sn^{4+}. A weighed amount of γ-Al_2O_3 was impregnated with the aqueous solution by the conventional incipient wetness technique. This paste was left to stand for 16 h. Aqueous solution of sodium borohydride (molar ratio of Ru + Sn to $NaBH_4$ 1:6) was added in drops to the aqueous slurry of the impregnated γ-Al_2O_3 support. After the reduction was complete, the solids were washed five times with distilled water and then finally with absolute alcohol. The solids were then air-dried and subjected to H_2 treatment under flowing conditions at 270°C for 2 h before carrying out any characterization. These are re-

---

[1] To whom all correspondence should be addressed.

[2] Present address: 11 The Grove, Lymm Cheshire, WA13 0HM, United Kingdom.

0021-9517/90 $3.00

ferred to as "fresh catalysts." This treatment corresponds to the reaction temperature of 270°C employed for most of the hydrogenation reactions reported in Part II (*11*).

Ru–Sn–B. The unsupported catalyst was prepared in the same manner as described above.

Ru–B and Ru–B/Al_2O_3. The monometallic borides were prepared in a manner similar to that described above.

$RuCl_3 \cdot 3H_2O$ was obtained from Fluka, Switzerland. Stannous chloride and sodium borohydride were procured from BDH, India, and were of 99% purity. γ-Al_2O_3 was supplied by Harshaw-Chemie, B.V., Netherlands and had a surface area of 200 m^2/g.

Chemical Analysis

Chemical analysis was carried out by means of inductively coupled plasma optical emission spectroscopy (ICPOES). The spectrometer used was a Jobin Yvon sequential spectrometer (Model JY-38, Division Instruments, France). Chloride was determined as silver chloride.

H_2 Chemisorption

H_2 chemisorption on the catalysts was carried out at 25°C after evacuating the system at 200°C to 10^{-4} Pa for 4 h using a conventional all-glass vacuum system. Before the adsorption isotherm was carried out, the samples were treated with H_2 at a pressure of 30 kPa at 100°C and degassed again at the same temperature to 10^{-4} Pa. The isotherms were then measured up to 40 kPa of H_2 at 25°C and the monolayer uptake was calculated by back-extrapolation to zero pressure.

X-Ray Photoelectron Spectroscopy

The photoelectron spectra were obtained with a Vacuum Generators ESCA 3 MK II spectrometer using monochromatic Al$K\alpha$ X rays (1486.6 eV). Pressure in the analyzer chamber during any run was less than 8×10^{-7} Pa. Binding energies were referenced to Al $2p$ (74.7 eV) in the case of γ-Al_2O_3-supported catalysts. In the case of unsupported catalysts, binding energies were referenced to the Au $4f_{7/2}$ (84.0 eV) line of a gold spot which had been evaporated onto the sample. In addition, the O $1s$ (532.3 eV) lines of the catalysts were employed as secondary internal standards. Quantification of the XPS spectra was carried out by taking the area ratios of the peaks. The areas were estimated by resolving the curves, assuming Gaussian peak shapes, and were corrected using cross sections reported by Scofield (*12*). Quantification of ruthenium peaks for alumina-supported catalysts could not be carried out because of poor resolution between ruthenium and carbon peaks. The spectra of the catalysts were recorded on fresh samples as well as after treatment with H_2 at 100°C. The *in situ* treatment with H_2 at 100°C within the spectrometer was carried out because it was felt that the catalysts pretreated in the H_2 flow at 270°C after $NaBH_4$ reduction might have undergone oxidation of the surface layers of the metal on exposure to air.

X-Ray Diffraction

XRD was carried out on a Philips 1700 series automatic powder diffraction system, using Cu$K\alpha$ radiation.

Transmission Electron Microscopy and Energy Dispersive X-Ray Analysis

The catalysts, ground in an agate pestle and mortar, were collected onto copper grids coated with a thin carbon film. The grids were examined in a Philips EM 400 electron microscope fitted with a field emission gun. Aggregate analysis was carried out on particles about 1 μm in size. Microarea analyses were carried out on small areas (200 Å^2) of these particles. The EDX data were processed with a Link systems AN 1000 computer using an RTS-2 software package.

Quantification of EDX Data: Triangular Diagrams

EDX analysis on the catalysts was quantified as follows. Aggregate and micro-area analyses were carried out on 10 different particles and 20 different areas, respectively, and the atomic percentages were plotted in a triangular diagram. The values for sensitivity factors for Ru and Sn were taken from the literature. All the elements were analyzed and normalized to 100% atomic weight. In the case of Ru–Sn–B, the triangular diagrams are at 100% in the corner of the element label; e.g., the label Ru is placed at the corner of 100% Ru. Ru, Sn, and the impurity silicon constitute the corners of the triangle. In the case of Ru–Sn–B/Al_2O_3 the corners of the triangle correspond to the elements Ru, Sn, and Al. The labels Ru and Sn are placed at the corners of 40% Ru and 40% Sn, respectively, while the label Al is placed at the corner of 100% Al (see Figs. 4 and 5).

Secondary Ion Mass Spectrometry

SIMS spectra of the samples were recorded with an I.S.A. Riber instrument (Rueil-Malmaison, France) in the positive ion mode using an energy selector, a quadrupole mass filter, a channeltron electron multiplier, and pulse counting electronics. The samples were powdered and pressed into disks. A 4-keV argon ion beam was used and ion currents were typically of the order of 1×10^{-10} Å/mm^2. Main chamber pressure during analysis was 10^{-6} Pa or less. No charge compensation was used. SIMS spectra of the samples were recorded after calibration using standard samples of metallic ruthenium powder and tin powder and physical mixtures of the two.

TABLE 1

Chemical Composition of the Catalysts

Catalyst	Composition (% by weight)					Atomic ratio
	Ru	Sn	B	Cl	Na	Sn/Cl
1. Ru–B	98	—	0.4	0.1	0.4	
2. Ru–Sn–B	28.5	30.1	0.4	0.2	0.8	45.1
3. Ru–B/Al_2O_3	1.1	—	0.2	0.1	0.3	
4. Ru–Sn–B/Al_2O_3	1.1	1.25	0.2	0.1	0.3	3.6

RESULTS

Chemical Composition

Table 1 gives the chemical composition of the catalysts. Since tin is not reduced with $NaBH_4$, the unsupported ruthenium–tin boride catalyst contains only 28.5% Ru and 30.1% Sn. Since the amount of chlorine is quite small, tin could be present as an oxide.

Degree of Dispersion of Ruthenium (from H_2 Chemisorption)

The data for the degree of dispersion, calculated from H_2 chemisorption, are presented in Table 2. It may be seen that on the unsupported catalysts, the degree of dispersion is rather low, indicating large average metal crystallites of ruthenium. Furthermore, there is only a marginal increase in the degree of dispersion on introduction of tin. However, the γ-alumina-supported catalysts show a fairly high degree of dispersion. Moreover, the introduction of tin increases the dispersion of ruthenium significantly (from 61 to 84%).

X-Ray Photoelectron Spectroscopy

Ru $3d_{5/2}$ spectra of Ru–B and Ru–Sn–B. It was found that the Ru $3d_{3/2}$ peak overlaps with the C 1*s* peak. Hence the Ru $3d_{5/2}$ peak was considered for all samples to find the binding energy.

TABLE 2

Degree of Dispersion of the Catalyst

Catalyst	Degree of dispersion (%)
1. Ru–B	10.0
2. Ru–Sn–B	13.0
3. Ru–B/Al_2O_3	61.0
4. Ru–Sn–B/Al_2O_3	84.0

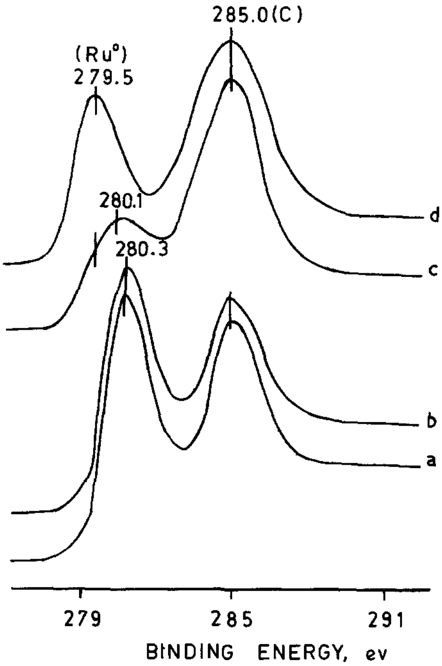

FIG. 1. XPS spectrum of Ru $3d_{5/2}$ for the catalysts Ru–B and Ru–Sn–B: (a) Ru–B (fresh), (b) Ru–B treated at 100°C with H_2, (c) Ru–Sn–B (fresh), (d) Ru–Sn–B treated at 100°C with H_2.

Figure 1 compares the Ru $3d_{5/2}$ spectra of the unsupported RuB and Ru–Sn–B catalysts treated at 100°C under H_2 as well as those of untreated samples. The binding energy values fall in the range of 279.5 to 280.1 eV and this can be ascribed to Ru^0 species in accordance with the literature (*13, 14*). The lower binding energy value of 279.5 eV in the case of Ru–Sn–B after hydrogen reduction can be explained by alkali metal in interaction with ruthenium. A similar observation was made by Mitchell *et al.* (*15*). XPS data (Table 3) show that the Na/Ru ratio on Ru–Sn–B is higher than that on Ru–B.

TABLE 3

Quantification of XPS Data

Catalyst	Atomic ratio from XPS			
	Sn/Cl	Sn/O	Na/Ru	Na/Al
1. Ru–B	—	—	0.02	—
2. Ru–Sn–B	17.5	0.4	0.03	—
3. Ru–B/Al_2O_3		—	—	0.004
4. Ru–Sn–B/Al_2O_3	5.2	0.11	—	0.04

Ru $3d_{5/2}$ spectra of RuB/Al_2O_3 and Ru–Sn–B/Al_2O_3. Figure 2 shows the Ru $3d_{5/2}$ spectra for the supported catalysts. Spectra a and b indicate that RuB/Al_2O_3 contains a mixture of Ru^{3+} and Ru^0 species. The shoulder at 280.5 eV is assigned to Ru^0 while the shoulder at 282.2 eV is assigned to Ru^{3+} in accordance with the literature (*13, 14*).

Spectrum c of the catalyst Ru–Sn–B/Al_2O_3 also shows two ruthenium species, Ru^0 and Ru^{3+}. (Although only one peak is seen at 280.1 eV, the asymmetric broadening of the peak is an indication of a second species.) Spectrum d shows a much narrower peak at 280 eV, indicating that this catalyst contains only Ru^0 species after H_2 treatment at 100°C.

XPS spectra of tin in the catalysts. Figure 3 shows the Sn $3d_{5/2}$ spectra of tin in the

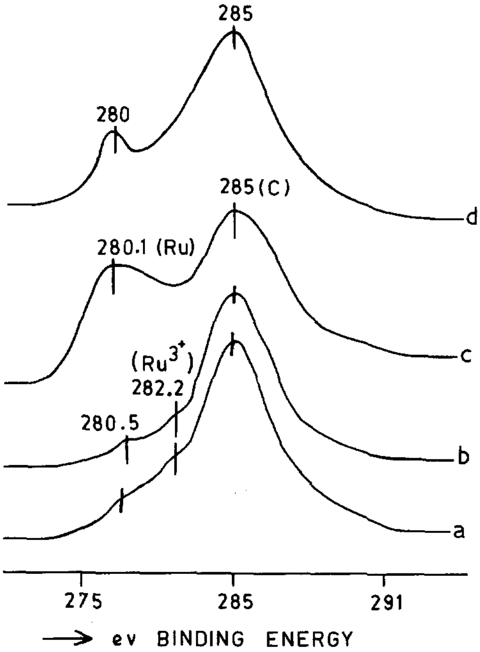

FIG. 2. XPS spectrum of Ru $3d_{5/2}$ for the catalysts Ru–B/Al_2O_3 and Ru–Sn–B/γ-Al_2O_3: (a) Ru–B/Al_2O_3 (fresh), (b) Ru–B/Al_2O_3 treated at 100°C with H_2, (c) Ru–Sn–B/Al_2O_3 (fresh), (d) Ru–Sn–B/Al_2O_3 treated at 100°C with H_2.

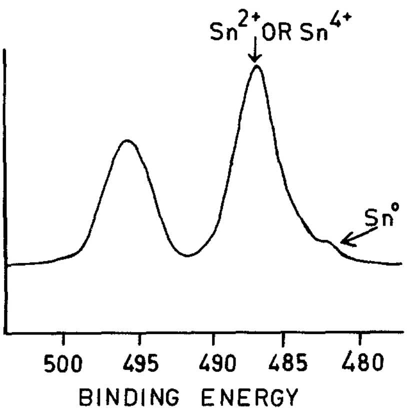

FIG. 3. XPS spectrum of tin in Ru–Sn–B.

catalyst Ru–Sn–B. The binding energy of 487.3 eV is consistent with Sn^{2+} or Sn^{4+} species. (The Sn 3*d* chemical shift between Sn^{2+} and Sn^{4+} is very small.) In addition to the major peak at 487.3 eV, the catalyst also shows a small shoulder at 484.0 eV, which may be assigned to Sn^0 in accordance with the literature (*16, 17*). The catalyst showed a similar spectrum after H_2 treatment at 100°C also.

The alumina-supported ruthenium–tin boride also showed a similar XPS spectrum for tin. Thus, on the mixed metal catalysts, tin exists predominantly as Sn^{2+} or Sn^{4+} and in small quantities as Sn^0 species.

Table 3 shows that the [Sn]/[Cl] values for Ru–Sn–B are too large for tin to exist as $SnCl_2$ or $SnCl_4$ on the surface. However, the corresponding ratios for tin to oxygen on the mixed metal catalysts suggest that tin may be present as oxide. This is quite understandable since the pH of the solution during sodium borohydride reduction is about 9. Chemical analysis results in Table 1, indicating high Sn/Cl ratios, also points to the same conclusion.

XPS of boron. The B 1*s* spectrum of the Ru–Sn–B catalyst showed a small signal which was located at 187.5 eV, in addition to the one at 192.0 eV. The former may be assigned to boron associated with ruthenium as ruthenium boride, in line with previous assignments on NiB, CoB, PtB, and PdB catalysts (*5–7*), while the latter corresponds to borate (B^{3+}) species. The B 1*s* spectrum of Ru–Sn–B/Al_2O_3 showed only one type of boron, predominantly at a binding energy of 192.0 eV. This may be attributed to boron in the oxidation state 3+ and may be present as sodium borate adsorbed on alumina. In addition, there was also a weak and noisy signal at 187 eV, probably due to ruthenium boride. No attempt was made to quantify the boron peaks.

TEM/EDX Analysis

TEM pictures were taken at a magnification of 90,000. EDX analysis was also carried out on these specimens. EDX of Ru–Sn–B and Ru–Sn–B/Al_2O_3 showed the presence of ruthenium as well as tin. The EDX spectra were quantified and the data are presented in the form of triangular diagrams in Figs. 4 and 5 for Ru–Sn–B and Ru–Sn–B/Al_2O_3, respectively. The details of the procedure adopted for quantification are described under Experimental.

In the case of the Ru–Sn–B catalysts, both aggregate analysis and micro-area analysis (Figs. 4a and b) show a spread for the ruthenium-to-tin ratio. The ratio ranges between 1 : 2 and 2 : 1 and the mean value for Ru : Sn is approximately 1 : 1. On the other hand, the supported catalyst, Ru–Sn–B/Al_2O_3, shows an undeniable trend to a fixed ratio for Ru : Sn of ~1 for both aggregate analysis and micro-area analysis (see Figs. 5a and b). This could be an indication of an interaction between Ru and Sn species.

In the case of the supported catalysts, however, the effect of dispersion must be considered. It is possible that a fixed Ru/Sn ratio is due to high dispersion, so even at 200 Å^2 area of analysis (in the case of micro-area analysis), a large number of primary particles may contribute. On the contrary, the dispersion is much lower for the unsupported catalyst, so the resolution of the microscope in the EDX analysis is

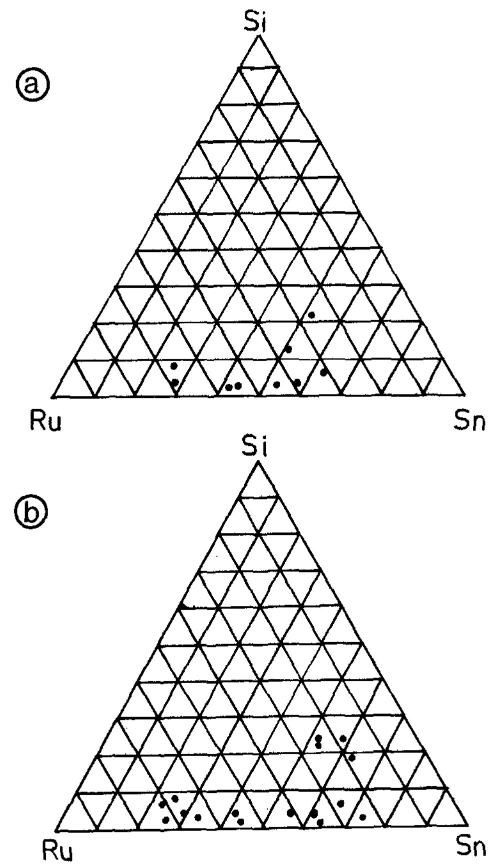

FIG. 4. Representation of EDX data as a triangular diagram for Ru–Sn–B catalyst. (a) Aggregate analysis. (b) Micro-area analysis.

enough to obtain a variation depending on the position on the sample.

While the EDX data cannot be taken as positive evidence for ruthenium–tin interaction on the supported catalysts, due to the effects of dispersion as discussed above, they could be considered as an indicator of an interaction at least for the unsupported catalyst since the area of analysis is as small as 200 Å^2. However, further confirmation of the interaction comes from XRD and SIMS data.

X-Ray Diffraction

The diffraction trace produced for the catalyst Ru–Sn–B before reduction with H_2 at 270°C showed extremely broad, diffuse diffraction maxima at $d = 3.5, 2.6, 2.1$, and 1.8 Å, suggesting that some ordering has started to take place in the specimen, but the widths of these maxima suggest that the material is essentially noncrystalline.

The catalyst Ru–Sn–B, after thermal treatment at 270°C under H_2 flow for 2 h, contained a fair proportion of noncrystalline material together with a major crystalline phase Ru_3Sn_7 and a possible trace of ruthenium metal.

The supported catalyst Ru–Sn–B/Al_2O_3 showed essentially the diffraction maxima corresponding to the γ-Al_2O_3 structure. There was no change in the XRD pattern even after heating to 270°C under H_2.

Secondary Ion Mass Spectroscopy

The SIMS spectrum of the catalyst Ru–Sn–B showed a number of peaks corre-

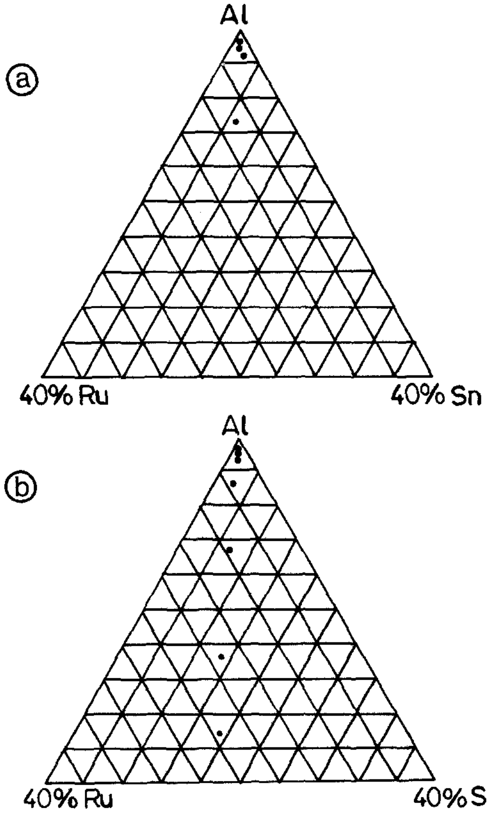

FIG. 5. Representation of EDX data as a triangular diagram for Ru–Sn–B/γ-Al_2O_3 catalyst. (a) Aggregate analysis. (b) Micro-area analysis.

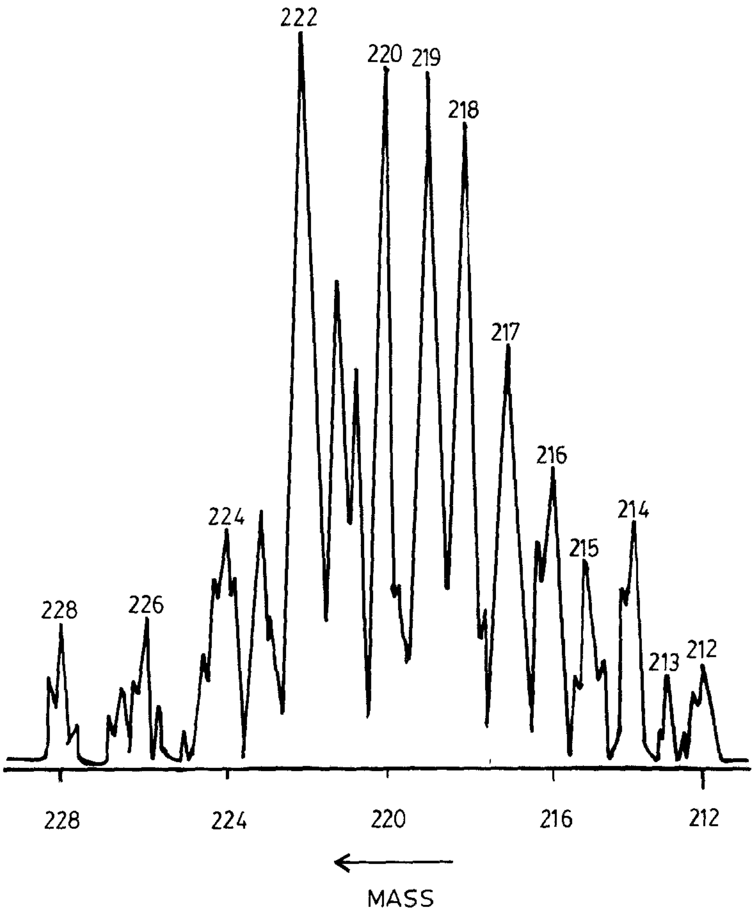

FIG. 6. SIMS spectrum of Ru–Sn–B catalyst.

sponding to Ru^+, Sn^+, $SnOH^+$, and also Na^+, Ca^+, and Sr^+. No attempt was, however, made to quantify these spectra. In Fig. 6 we show that portion of the SIMS spectrum which is of interest. It may be observed that a bunch of lines lie between the mass numbers 212 and 228. These peaks correspond to $SnRu^+$ species. We further calculated the possible isotope pattern for the Sn–Ru (1 : 1) system, based on the abundance of isotopes, and this is shown in Fig. 7. The numbers on the top are the relative intensities of the peak normalized with respect to the most intense peak at 220. Although the intensity pattern in Fig. 6 does not exactly match that expected theoretically, there is reasonable similarity between the two figures. SIMS spectra of different physical mixtures of ruthenium metal powder and tin (as SnO and metal powder) were taken and it was found that they did not show any peaks in the mass range 212–228. This rules out any possibility of recombination of ions during the SIMS analysis for the catalyst samples studied. Thus, the similarity of Figs. 6 and 7 may be taken as evidence for interaction between ruthenium and tin species.

The SIMS spectra for Ru–Sn–B/Al_2O_3 showed small peaks due to $SnAl^+$ and $RuAl^+$, indicating signs of interaction between the metals and the support. No peaks due to $SnRu^+$-type species were observed, presumably because ruthenium and tin may be interacting strongly with the alumina support which is present in abundance.

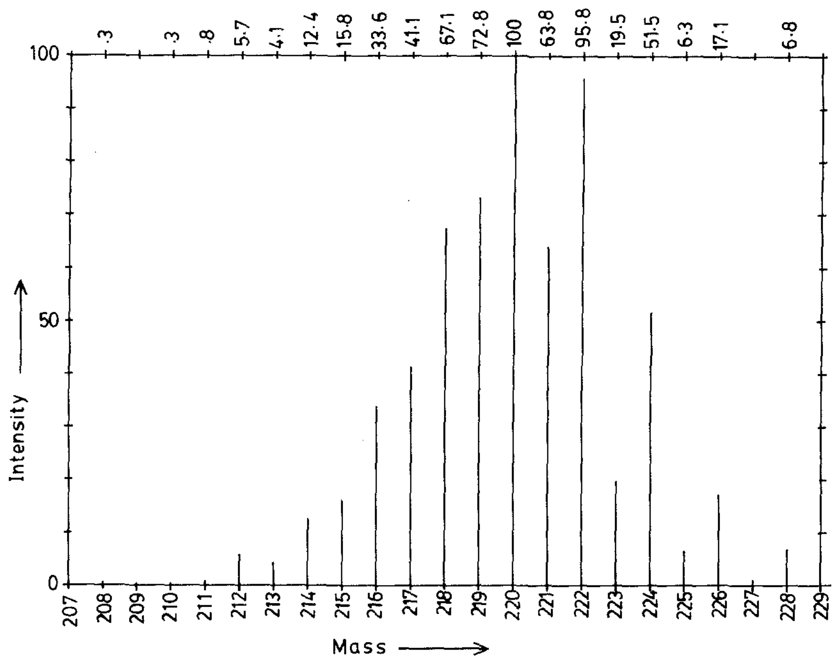

FIG. 7. Calculated SIMS pattern for Ru–Sn mixture (1 : 1) based on isotope abundance.

Furthermore, the concentration of species such as $SnRu^+$ could be quite small relative to the unsupported catalyst due to high dispersion and very small metal loading (~1.1%).

DISCUSSION

Ru–Sn–B

The XPS studies have clearly shown that ruthenium is present as Ru^0 in the Ru–Sn–B system (supported and unsupported), while tin exists in two oxidation states: Sn^{2+} or Sn^{4+} in major concentration and Sn^0 in minor quantities. Since the concentration of chlorine is quite small and oxygen was found in significant amounts, tin must be present predominantly as tin oxide. XPS also shows the presence of boron as boride partly. Moreover, while ruthenium–tin interaction is indicated by EDX analysis, SIMS data provide the confirmatory evidence of the interaction. We believe that the presence of Ru and Sn species shown by SIMS and EDX is due primarily to interacting of Ru^0 with Sn=O

$$B \rightarrow Ru^0 \; . \; . \; . \; . \; . \; O{=}Sn \quad \text{(type I site).}$$

This picture also fits the observation by XPS that tin is present predominantly as Sn^{2+} and Sn^{4+} on the surface. Such sites could also explain the increase in dispersion of ruthenium on addition of tin, the effect being due to SnO's acting as a spacer between Ru^0 sites. Boron is shown to be associated with ruthenium in the type I site, in accordance with XPS evidence of the presence of boride. Thus, the XRD evidence of a possible alloy formation (Ru_3Sn_7) should correspond primarily to the bulk of the catalyst. However, one cannot rule out such sites as

$$B \rightarrow Ru{-}Sn{-}Ru \quad \text{(type II site)}$$

on the surface (at least in relatively small concentration) in view of XPS evidence for minor quantities of tin present as Sn^0.

Ru–Sn–B/Al₂O₃

While the above hypothesis regarding surface species is essentially made for the unsupported catalysts, it is reasonable to extrapolate this picture to the supported catalysts as well (although there is no positive spectroscopic evidence), for the following reasons. (1) As already pointed out, due to the high degree of dispersion and the resultant very low concentration of $SnRu^+$-type species, SIMS may not show up such mass ions. (2) The supported and the unsupported mixed metal catalysts behave in an amazingly similar fashion toward various reactants for hydrogenation [see Part II (*11*)].

CONCLUSIONS

1. Ruthenium–tin boride prepared by sodium borohydride reduction is suggested to form two types of site: (a) Ru^0 interacting with Sn^{2+} or Sn^{4+} via the oxygen; (b) alloy type (Rn_3Sn_7), wherein ruthenium as well as tin is present in zero oxidation state (this may be present in small quantities on the surface).
2. Boron is present as borate ($Na_2B_4O_7$) as well as boride associated with ruthenium.
3. Tin, present as SnO, increases ruthenium metal dispersion.

ACKNOWLEDGMENT

We thank ICI, India, Limited for financial support.

REFERENCES

1. Wade, R. C., *J. Mol. Catal.* **18,** 273 (1983).
2. Midland, M. M., and Lee, P. E., *J. Org. Chem.* **50,** 3237 (1985).
3. Hutchinson, C. R., Heckendorf, A. H., Straughn, J. L., Daddona, P. E., and Cane, D. E., *J. Amer. Chem. Soc.* **101,** 3358 (1979).
4. Satoh, T., Suzuki, S., Kikuchi, T., and Okada, T., *Chem. Ind.*, 1626 (1970).
5. Okamoto, Y., Nitta, Y., Imanaka, T., and Teranishi, S., *J. Chem. Soc., Faraday Trans. I* **75,** 2027 (1979).
6. Okamoto, Y., Nitta, Y., Imanaki, T., and Teranishi, S., *J. Catal.* **64,** 397 (1980).
7. Okamoto, Y., Fukuro, K., Imanaka, T., and Teranishi, S., *J. Catal.* **74,** 173 (1982).
8. Wade, R. C., Holah, D. G., Hughes, A. N., and Hui, B. C., *Catal. Rev. Sci. Eng.* **14,** 211 (1976).
9. Narasimhan, C. S., Deshpande, V. M., and Ramnarayan, K., *J. Chem. Soc. Chem. Commun.*, 99 (1988).
10. Narasimhan, C. S., Deshpande, V. M., and Ramnarayan, K., Indian Patent Application No. 570/Cal/1987 and 571/Cal/1987.
11. Deshpande, V. M., Ramnarayan, K., and Narasimhan, C. S., *J. Catal.* **121,** 174 (1990).
12. Scofield, J. H., *J. Electron Spectrosc.* **8,** 129 (1976).
13. Kim, K. S., and Winograd, N., *J. Catal.* **35,** 66 (1974).
14. Aika, K., Ohya, A., Ozaki, A., Inoue, Y., and Yasumori, I., *J. Catal.* **92,** 305 (1985).
15. Mitchell, P. C. H., Scott, C. E., Bonnelle, J. P., and Grimblot, J. G., *J. Catal.* **107,** 482 (1987).
16. Grutsch, P. A., Zeller, M. V., and Fehlner, T. P., *Inorg. Chem.* **12**(6), 1431 (1973).
17. Ansell, R. O., Dickinson, T., Povey, A.F., and Sherwood, P. M. A., *J. Electron. Spectrosc. Relat. Phenom.* **11,** 301 (1977).